available at www.sciencedirect.com

SCIENCE DIRECT®

journal homepage: www.elsevier.com/locate/biochempharm

Peptide-bond modified glutathione conjugate analogs modulate GSTπ function in GSH-conjugation, drug sensitivity and JNK signaling

Danny Burg, Joey Riepsaame, Chantal Pont, Gerard Mulder, Bob van de Water *

Division of Toxicology, Leiden/Amsterdam Center for Drug Research, Leiden University, P.O. Box 9502, 2300 RA Leiden, The Netherlands

ARTICLE INFO

Article history:
Received 25 August 2005
Accepted 2 November 2005

Keywords:
Glutathione S-transferase
Peptidomimetic
Multidrug resistance
cJun N-terminal kinase
Glutathione conjugate
Cytostatics

ABSTRACT

Glutathione S-transferase π (GST, E.C.2.5.1.18) overexpression contributes to resistance of cancer cells towards cytostatic drugs. Furthermore, GSTπ is involved in the cellular stress response through inhibition of Jun N-terminal-kinase (JNK), a process that can be modulated by GST inhibitors. GSH conjugates are potent GST inhibitors, but are sensitive towards γ-glutamyltranspeptidase (γGT)-mediated breakdown. In search for new peptidase stable GST inhibitors we employed the following strategy: (1) selection of a suitable (GST inhibiting) peptide-bond isostere from a series of previously synthesized γGT stabilized GSH-analogs. (2) The use of this peptidomimetic strategy to prepare a GSTπ selective inhibitor. Two γGT stable GSH conjugate analogs inhibited human GSTs, although non-selectively. One of these, a urethane-type peptide-bond is well accepted by GSTs and we selected this modification for the development of a γGT stable, GSTπ selective inhibitor, UrPhg-Et_2. This compound displayed selectivity for GSTπ compared to α and μ class enzymes. Furthermore, the inhibitor reversed GSTπ-mediated drug resistance (MDR) in breast tumor cells. In addition, short-term exposure of cells to UrPhg-Et_2 led to GSTπ oligomerization and JNK activation, suggesting that it activates the JNK-cJun signaling module through GSTπ dissociation. Altogether, we show the successful use of peptidomimetic glutathione conjugate analogs as GST inhibitors and MDR-modifiers. As many MDR related enzymes, such as MRP1, glyoxalase 1 and DNA-pk are also inhibited by GSH conjugates, these peptidomimetic compounds can be used as scaffolds for the development of multi-target MDR drugs.

1. Introduction

Glutathione S-transferases (GSTs, E.C.2.5.1.18) play a pivotal role in the protection of cells from injury by toxic chemicals [1–4]. GSTs conjugate xenobiotic or endogenously formed electrophiles with the abundant tripeptide glutathione (γ-L-glutamyl-L-cysteinyl-glycine, GSH). The mammalian GST family consists of eight distinct classes of cytosolic/mitochondrial and four classes of membrane-bound (microsomal, MAPEG) GST isoenzymes [5,6], which have different, but partially overlapping substrate specificity towards electrophilic substrates. Overexpression of α, μ and π class cytosolic GSTs has been associated with resistance of tumor tissues to cytostatic drugs [7], although various studies have shown that GST overexpression by itself is not sufficient to generate a multidrug resistant phenotype. Increased efflux of the formed GSH conjugates by overexpression of multidrug resistance associated protein (MRP1) is often also required [8]. GST is

* *Corresponding author*. Tel.: +31 715276223.
E-mail address: b.water@lacdr.leidenuniv.nl (B. van de Water).
0006-2952/$ – see front matter © 2005 Elsevier Inc. All rights reserved.
doi:10.1016/j.bcp.2005.11.003

thought to protect by direct detoxification of electrophilic species, or by inactivation of reactive intermediates formed during treatment with cytotoxic agents [9,10]. Furthermore, GSTs were shown to regulate stress-activated signal transduction pathways: cJun NH_2-terminal kinase (JNK/SAPK), which plays a crucial role in both cell-survival and death pathways, is partly regulated by protein–protein interactions with GSTπ [10,11]. Similar functions in regulating stress-activated signaling kinases have also been reported for other GST family members. GSTμ, for example, mediates the activity of Ask1 and MEKK1 [12,13], two upstream components of the JNK/SAPK signaling pathway. GSTω, in addition, regulates ryanodine receptors, which are main regulators of calcium homeostasis [12]. As ryanodine receptor mediated release of Ca^{2+} from internal stores precedes many crucial cellular processes, GSTω may also have a regulatory function.

Altogether, these findings show that GST inhibitors, besides their ability to modulate GST-mediated GSH-conjugation, can also influence cell signaling processes [14]. The use of such compounds is illustrated by TLK199, an isoenzyme selective GSTπ inhibitor that is able to increase the cytostatic effect of anti-cancer agents [15]. In addition, TLK199 initiates a signal transduction cascade by dissociating GSTπ from JNK, which subsequently phosphorylates its downstream target cJun [10]. In vivo, this process leads to increased myeloproliferation, which is currently being explored in a clinical setting. These studies emphasize the importance of GST inhibitors as pharmacological manipulators of signaling cascades.

GSH conjugates are commonly good inhibitors of GSTs in vitro [16–18]. Although the γ-glutamyl-cysteine peptide-bond renders them resistant to most α-peptidases, GSH conjugates are rapidly degraded by γ-glutamyl transpeptidase (γGT) [19]. Cleavage by this enzyme, which has particularly high activity in the kidney, precludes the use of GSH conjugates in vivo [20]. Recently, we synthesized a series of novel peptidomimetic GSH conjugate analogs (Fig. 1) [21], some of which were stabilized towards γGT-mediated breakdown. These GSH-isosteres were conjugated to ethacrynic acid [22,23], thus enabling us to evaluate the effect of peptide-backbone modification on GST inhibition. Initial studies indicated that these compounds inhibit GST activity in the rat liver S100 fraction, a mixture of mainly α and μ class GSTs [21]. As GSH conjugates are also good MRP1 inhibitors, our series of GS-EA analogs was also tested for MRP1 inhibition. We showed that our new peptidomimetics modulate resistance towards methotrexate in MRP1 overexpressing ovarian carcinoma cells [24]. In the current report, we characterize the GST inhibition by peptidomimetic GS-EA analogs on human GST isoenzymes to find a peptide-bond mimetic that is compatible with GST inhibition. We selected a urethane-type peptide-bond isostere for the design of a novel GSTπ inhibitor, UrPhg and its cell permeable diethyl ester derivative, UrPhg-Et_2. We find that the novel compound increases sensitivity of mammary carcinoma cells towards cytostatics. In addition, UrPhg-Et_2 initiates a JNK-mediated signal transduction cascade, leading to phosphorylation of the transcription factor cJun. Altogether, the data indicate that peptide-bond modified GSH conjugates can be used to modulate various cellular processes, such as GSTπ-mediated MDR and MAP-kinase signaling.

2. Materials and methods

2.1. Materials

Recombinant human GST isoenzymes A1-1, M1-1 and P1-1 were purchased from PanVera Corporation (Madison, WI, USA). Cisplatin, thiotepa and doxorubicin were obtained from Sigma (St. Louis, MO, USA). GST assays were performed in 96-well plates using a Perkin-Elmer HTS7000 BioAssay Reader (Perkin-Elmer, Boston, MA, USA). Phospho-state specific antibodies, were obtained from Cell Signaling (Beverly, MA, USA).

2.2. Cell lines

VCREMS and MCF7 human mammary carcinoma cells, were cultured in DMEM, supplemented with 10% (v/v) fetal calf serum, 100 U/l penicillin and 100 mg/l streptomycin. MTLn3 rat mammary adenocarcinoma cells were grown in Mem-α, supplemented with 5% (v/v) fetal calf serum. All cells were cultured at 37 °C in a humidified 5% CO_2 atmosphere.

2.3. Synthesis of GSH conjugate analogs

γ-Glutamyl-(*S*-benzyl)cysteinyl-phenylglycine (γGCP, identical to TLK199), was synthesized according Lyttle et al. [25]. The synthesis of peptidomimetic GS-EA analogs was recently described [21]. Cys(EA)–Gly was synthesized in accordance with these published methods. Non-esterified, phenylglycine containing, compounds were obtained by similar methods described in our original article [21]; deviations from these protocols are the use of phenylglycine-OtBu, instead of glycine-OtBu and *S*-alkylation with benzylbromide, instead of ethacrynic acid (see Fig. 3A). Synthesis of the diethylester derivatives was performed using serine ethyl ester, phenylglycine ethyl ester [25] and *S*-benzylcysteine as building blocks (Fig. 3B). All compounds were purified by HPLC, using a separations system (Separations Analytical Instruments, Hendrik Ido Ambacht, The Netherlands) equipped with a Supelcosil SPLC-18-DB semi-preparative column and UV-detection (Waters 490 detector) at 254 nm. A linear gradient (10–95%) acetonitrile in H_2O/0.1% TFA was used to purify end products. All tested compounds were >95% pure, as determined by HPLC (column: Alltech Platinum C18, Alltech, Breda, The Netherlands, UV detection at 210/254 nm) and LC–MS (Alltech Platinum C18 column, Perkin-Elmer Sciex API 165 mass spectrometer).

2.4. Inhibition of recombinant GST isoenzymes

GST inhibition assays were performed according to Habig et al. [26], modified for a 96-wells plate-reader. Recombinant GSTs (10–20 ng/ml) were incubated with or without inhibitor in the presence of 1 mM GSH at 37 °C in 0.1 M potassium phosphate buffer pH 6.5, containing 1 mM EDTA. For the determination of IC_{50} values, six different inhibitor concentrations were tested (range 1–500 μM, depending on inhibitor efficacy). The reaction was initiated by addition of 1-chloro-2,4-dinitrobenzene (CDNB) in ethanol (final concentration 1 mM, 2% ethanol in assay mix), after which the formation of GS-DNB was spectrophotometrically monitored at 340 nm. Reaction rates

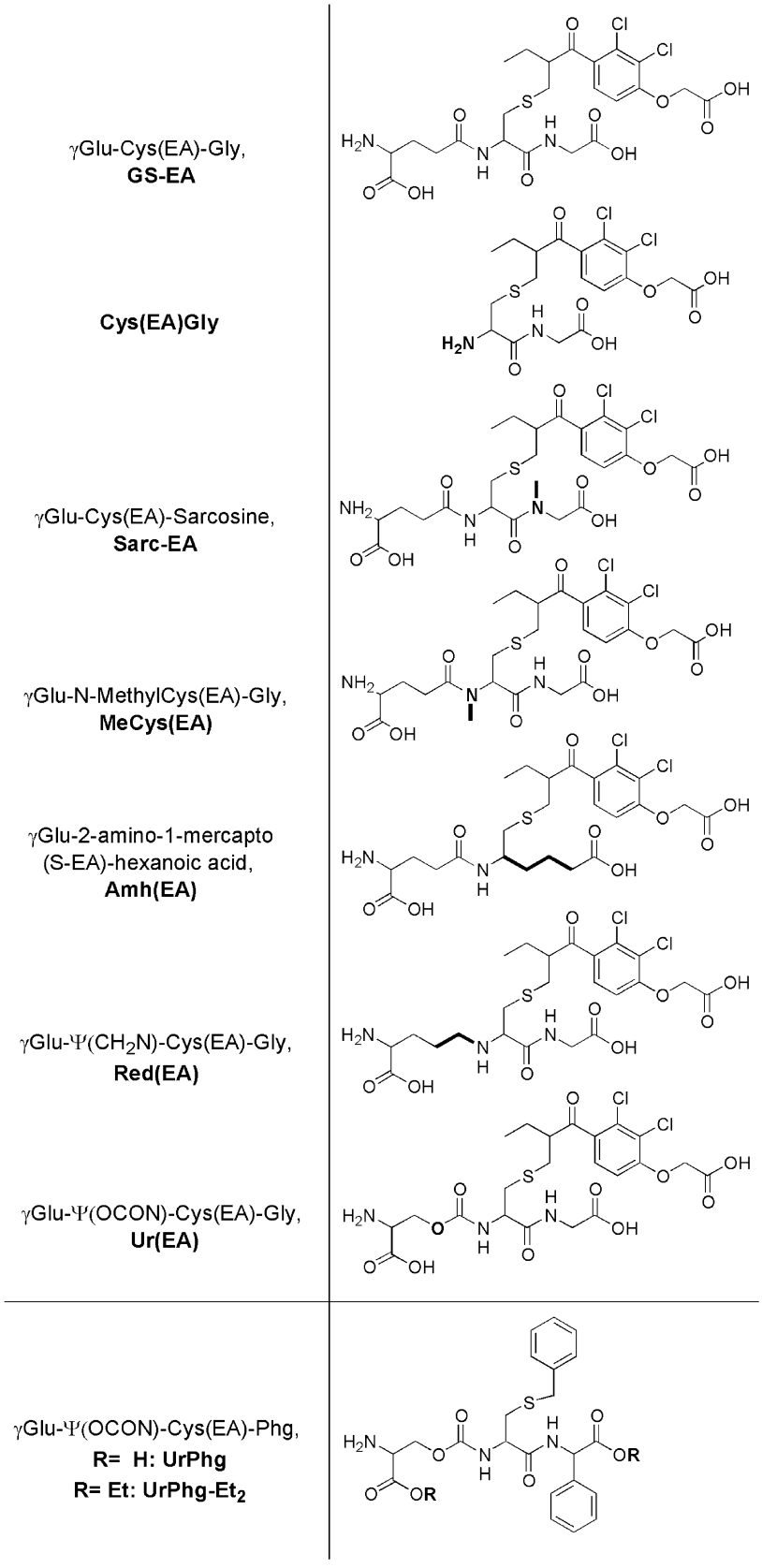

Fig. 1 – Peptide-bond modified GSH conjugate analogs. Deviations from the GSH-backbone are indicated in bold.

were corrected for the non-enzymatic conjugate formation. IC_{50} values were obtained by non-linear regression of the inhibition data. Experiments were performed three times, using quadruple samples per data point. Kinetic parameters of GSTA1-1, GSTM1-1 and GSTP1-1 inhibition by GS-EA analogs were determined at various GSH concentrations (0.1–4 mM) with constant CDNB (1 mM). K_i values were obtained by the $K_{m,app}$ method described by Kakkar et al. [27,28]. From the [S] versus V_0 curves, apparent K_m and V_{max} values were obtained by non-linear regression (Graphpad Prism, Graphpad Software, San Diego, CA, USA). The K_i value was determined by extrapolation of the linear K_m/V_{max} versus [inhibitor] graph.

2.5. Immunoblotting

Confluent monolayers of MTln3 cells in 6-well culture dishes were exposed to UrPhg-Et_2 in complete medium at 37 °C. Cells were then washed, scraped in ice-cold PBS and subsequently lysed by ultrasonication in cold TSE (10 mM Tris, 250 mM sucrose, 1 mM EGTA, pH 7.4), containing protease inhibitors (50 mM Na_3VO_4, 10 μg/ml leupeptin, 10 μg/ml pepstatin, 1 mM phenylmethylsulfonylfluoride). For GSTπ blotting, non-reducing and non-denaturing conditions were employed to maintain its original (homodimer) state. (Phospho)JNK, (phospho)Erk, (phospho)P38 and (phospho)cJun blots were subjected to standard Western blotting sample pre-treatment protocols. Twenty micrograms of total cellular protein was separated by SDS-polyacrylamide gel electrophoresis and subsequently transferred to PVDF membrane (Millipore, Billerica, MA, USA). Blots were blocked with 5% BSA in TBS-T (0.5 M NaCl, 20 mM Tris–HCl, 0.05%, v/v Tween 20; pH 7.4) and probed for the appropriate proteins. The secondary HRP-coupled antibody was visualized with ECL reagent (Amersham Pharmacia Biotech, Piscataway, NJ, USA).

2.6. Antineoplastic drug cytotoxicity assays

MCF7 and VCREMS cells were seeded at 4×10^3 cells/well in 96-wells polyethylene culture dishes. After overnight attachment, culture medium was replaced by Hanks' Balanced Salt Solution (HBSS: 137 mM NaCl, 5 mM KCl, 0.8 mM $MgSO_4$, 0.4 mM Na_2PO_4, 0.4 mM KH_2PO_4, 1.3 mM $CaCl_2$, 4 mM $NaHCO_3$, 25 mM HEPES, 5 mM D-glucose; pH 7.4), containing the GST inhibitor and various concentrations of cytostatic agents (from freshly prepared DMSO stock solutions, maximal DMSO concentration in final incubation volume 0.3%, v/v). Experiments were performed three separate times with each point determined in quadruple. After 4 h at 37 °C, cells were washed twice with PBS, and subsequently incubated for 72 h in complete culture medium (in absence of inhibitor). The cells were then rinsed once with PBS and lysed by repeated freeze–thaw cycles in 200 μl water, followed by homogenization on a rotary shaker. Cell proliferation was measured by DNA content, using Hoechst-33258 staining according to Rago et al. [29]. In short: 50 μl Hoechst-33258 (20 μg/ml in TNE; 10 mM Tris, 1 mM EDTA, 0.2 M NaCl, pH 7.4) was added to 50 μl lysate. Stained DNA was measured by spectrofluorometry (excitation: 360 nm; emission 465 nm). A calibration curve of calf thymus DNA was used to determine total DNA quantities. Growth curves were calculated using Graphpad/Prism.

Table 1 – Inhibition of human GST isoenzymes by GS-EA mimics

Inhibitor	IC_{50} (μM)		
	GSTA1-1	GSTM1-1	GSTP1-1
GS-EA	2.3 ± 0.1	0.6 ± 0.2	4.5 ± 0.6
Cys(EA)–Gly	>500	>500	>500
Sarc(EA)	4.5 ± 0.2	7.6 ± 0.7	4.8 ± 0.4
MeCys(EA)	>500	53 ± 8	>500
AmHex(EA)	>500	61 ± 5	390 ± 20
Red(EA)	37 ± 3	12 ± 2	45 ± 2
Ur(EA)	8.5 ± 1.4	6.7 ± 0.8	28 ± 4

Shown are inhibitor concentrations at which half-maximal enzyme activity was obtained (IC_{50}, mean ± S.E.M., $n = 4$).

3. Results

3.1. Inhibition of human GSTs

Many alterations to the GSH peptide backbone have been made, mainly by substitution of the amino acids; modifications of the internal peptide-bonds have rarely been made [30]. We used peptide-bond surrogates to potentially improve inhibition characteristics and peptidase stability. To compare the inhibition of human GST isoenzymes, IC_{50} values were obtained for the series of GS-EA analogs (Table 1). IC_{50} values could not be determined for Cys(EA)–Gly as hardly any inhibition was measured at 500 μM, indicating that the γ-Glu portion is critical for binding efficiency. *N*-Methylation of the Cys–Gly amide is very well accepted by GSTA1-1 and GSTP1-1. Interestingly, inhibition of GSTM1-1 is decreased by this methylation. Contrary to methylation of the Cys–Gly-bond, *N*-methylation of the γ-glutamyl peptide-bond in MeCys(EA) is not accepted by these enzymes. Apparently, the increased steric bulk prevents this compound from binding to the GST G-site. The increased flexibility and the loss of H-bonds by omission of the Cys–Gly peptide-bond in Amh(EA) prevent the compound from binding correctly. The reduced isostere, Red(EA) has lost some of its activity on the human GSTs, but is still able to interact with the enzymes. The urethane derivative Ur(EA) is a fairly good inhibitor of GSTA1-1, being four-fold less potent than GS-EA.

We next investigated the inhibition characteristics of two γGT stable compounds, Red(EA) and Ur(EA) in more detail. As differences in inhibition are presumably a result of altered binding in the GST G-site, we determined inhibitory constants towards GSH. As shown by Lineweaver–Burk plots (Fig. 2), the two compounds inhibit GSTM1-1 and GSTP1-1 competitively; GSTA1-1 displays a mixed-type inhibition. These data suggest that the inhibitors compete with GSH for binding the G-site. Ur(EA) is a more potent inhibitor of the human GST isoenzymes than the reduced isostere, Red(EA). Both compounds inhibited GSTM1-1 equally well, but K_i values (Table 2) indicate a reduction in affinity compared to unmodified GSH. GSTP1-1 required higher concentrations for inhibition.

Altogether, data indicate that the reduced and urethane peptide-bond isosteres are well accepted by human α, μ and π class GSTs. Red(EA) and Ur(EA) can be regarded as lead compounds for the development of novel, γGT stabilized GST inhibitors. As a next step we, therefore, investigated whether

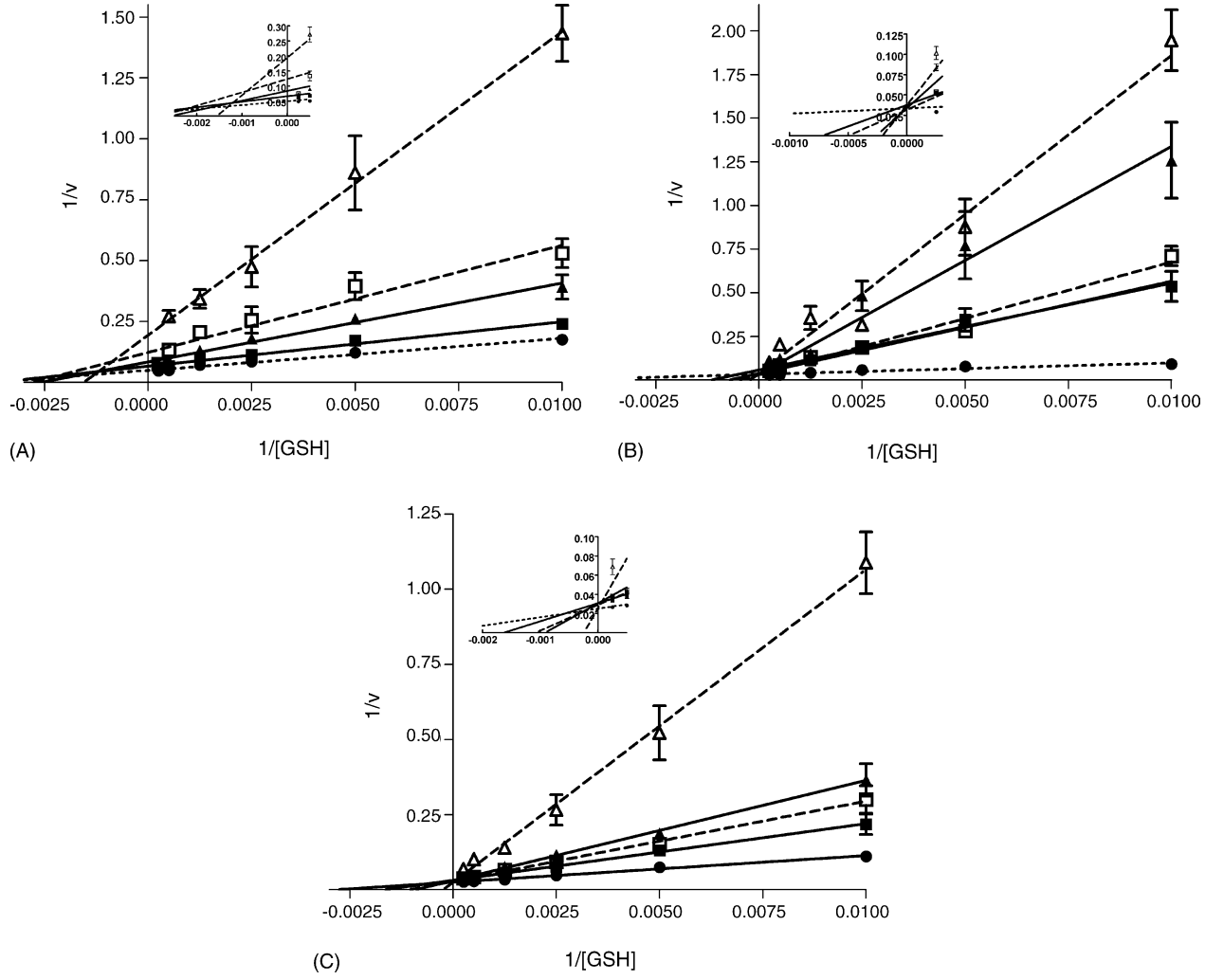

Fig. 2 – Lineweaver–Burk representation of inhibition of human GSTs by Red(EA) and Ur(EA). Shown are reciprocal enzymatic velocities (±S.E.M., *V* in μmol/min/mg protein) vs. 1/[GSH] (μM^{-1}) of GSTA1-1 (A), GSTM1-1 (B) and GSTP1-1 (C) without inhibitor (- - -), or with Red(EA) (—) or Ur(EA) (– – –). *Symbols*: (●) no inhibitor; (■) Red(EA) 10 μM; (▲) Red(EA) 50 μM; (□) Ur(EA) 12.5 μM; (△) Ur(EA) 25 μM. Insets represent a magnified view of the graph.

the urethane peptide-bond isostere could be used in the design of a more selective GSTπ inhibitor.

3.2. *Synthesis and evaluation of a phenylglycine containing GST inhibitor*

To date, the most potent competitive, isoenzyme selective GSTπ inhibitor is TLK199. This compound contains a phenylglycine moiety that interacts with a hydrophobic pocket near the GSTπ GSH binding site [31]. TLK199 owes its selectivity to the absence of this lipophilic cavity in other GST classes. To gain selectivity for GSTπ we utilized this moiety, together with TLK199's benzyl thioether, to obtain selective peptidomimetic inhibitors. For the synthesis of the non-esterified phenylglycine-containing urethane analog, UrPhg, shown in Fig. 3A, we essentially employed methods analogous to the synthesis of Ur(EA) [21]. In short, acylation of BocSerOtBu with bis(4-nitrophenyl)carbonate yields an *o*-nitrophenyl building block, which is condensed with Cys(Acm)–PhgOtBu. After removal of the Acm group, the benzyl thioether function can be attached at the last synthesis step, which is useful for screening various thioether moieties. During synthesis, we observed racemization of the phenylglycine moiety, as was also described for TLK199 [32]; the L- and D-phenylglycine containing products were separated by semi-preparative HPLC. Overall purity of the D-phenylglycine product, the major peak eluting later from the column, was approximately 90%. The L-phenylglycine product could not be

Table 2 – K_i values for inhibition of human GST isoenzymes by GSH conjugate analogs

Inhibitor	K_i values (μM)		
	GSTA1-1	GSTM1-1	GSTP1-1
Red(EA)	16 ± 3	6 ± 3	22 ± 6
Ur(EA)	4 ± 2	3 ± 1	16 ± 7
UrP-Bzl	29 ± 4	16 ± 2	3 ± 2

K_i values (mean ± S.E.M., $n = 3$) were obtained by non-linear regression of Michaelis–Menten graphs.

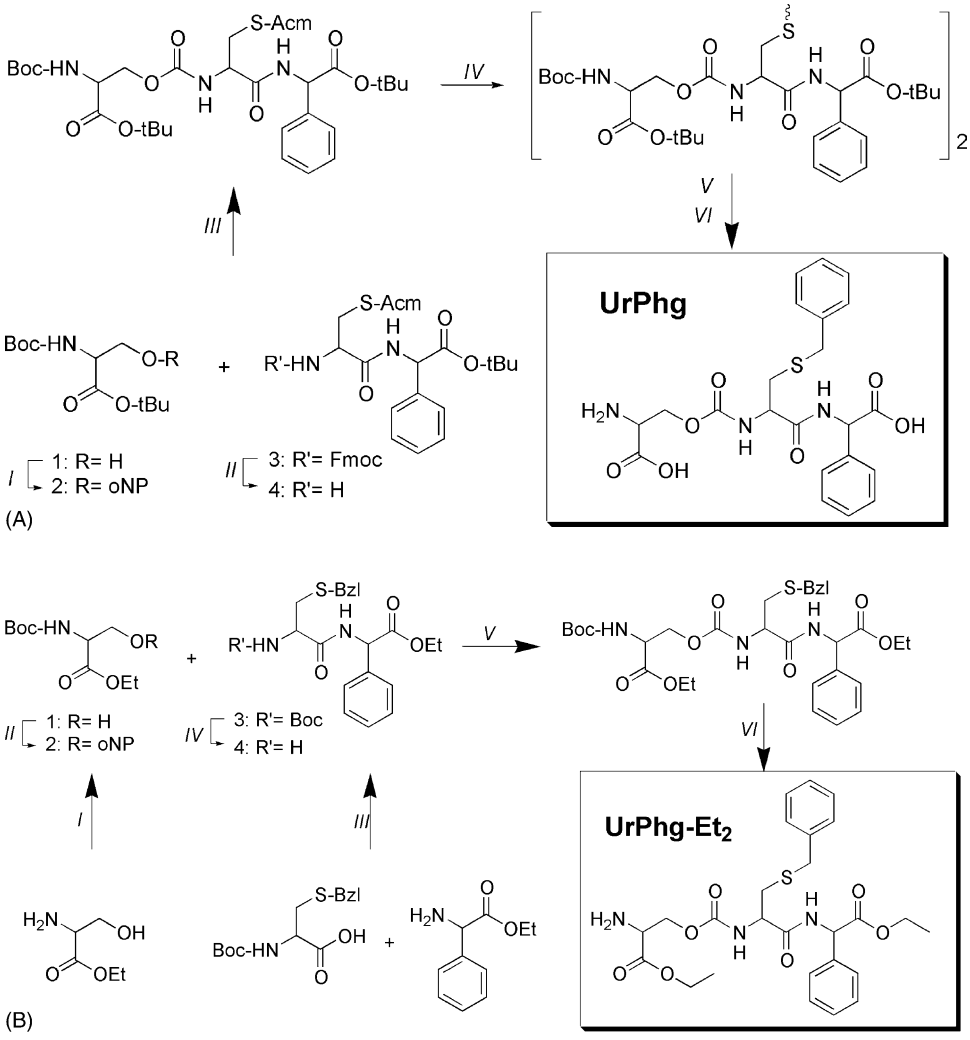

Fig. 3 – (A) Synthesis of UrPhg: (I) bis(4-nitrophenyl)carbonate, diisopropylethylamine (DiPEA), dimethylformamide (DMF); (II) 1,8-diazabicyclo[5.4.0]undec-7-ene (DBU), dichloromethane (DCM); (III) dioxane, 80 °C; (IV) I_2, methanol (MeOH); (V) trifluoroacetic acid (TFA)/H_2O (98:2, v/v); (VI) tri-*n*-butylphosphine, *n*-propanol/H_2O (3:1, v/v), benzylbromide, sodiumbicarbonate, EtOH/H_2O. (B) Synthesis of UrPhg-Et_2: (I) di-*tert*-butyldicarbonate (Boc_2O), triethylamine; (II) bis(4-nitrophenyl)carbonate, DiPEA, DMF (III) dicyclohexylcarbodiimide (DCC), hydroxybenzotriazole (HOBt), DCM; (IV) TFA/DCM (3:7); (V) dioxane, 80 °C; (VI) TFA/DCM (3:7).

obtained in acceptable purity. Initial inhibition experiments indicated that the D-phenylglycine product is a better GSTπ inhibitor than its L-diastereomer (not shown); we only use the D-product for our inhibition studies. UrPhg competitively inhibits GSTA1-1, GSTM1-1 and GSTP1-1. K_i values (Table 2) indicate that inclusion of the phenylglycine moiety indeed provides selectivity for the π class enzyme. UrPhg is a fairly potent GST inhibitor, displaying 4–10 fold selectivity for GSTP1-1 over the μ and α class enzymes. Although potent, UrPhg is a weaker GSTπ inhibitor than parent compound TLK199, for which literature data and our own inhibition data show a submicromolar (<1 μM) K_i [33].

For cell-based assays, the charged carboxylate residues of UrPhg have to be shielded by esters, as this dramatically improves their cellular uptake [34]. Initial attempts to obtain the diethyl ester derivative of UrPhg, UrPhg-Et_2, using SOCl or TMS-Cl in dry ethanol failed due to the generation of numerous by-products. Thus, we employed a more direct method, shown in Fig. 3B, to obtain UrPhg-Et_2. Starting from D-phenylglycine-ethyl ester, *S*-benzyl cysteine and serine-ethyl ester, we constructed the diester derivative according to our published methods [21]. The end-product was purified in good yield without significant racemization, due to the use of Boc-protected cysteine instead of Fmoc. We used the diethyl ester derivative to evaluate the effects of GSTπ inhibition on GSTπ-mediated drug resistance in breast tumor cells and on the MAPK signaling pathways.

3.3. *UrPhg-Et_2 induces GSTπ oligomerization and MAPkinase signaling*

GSTπ inhibitors can dissociate the GSTπ/JNK complex [10]. In line with these studies, we investigated whether UrPhg-Et_2 induces GSTπ oligomerization and activation of JNK signaling

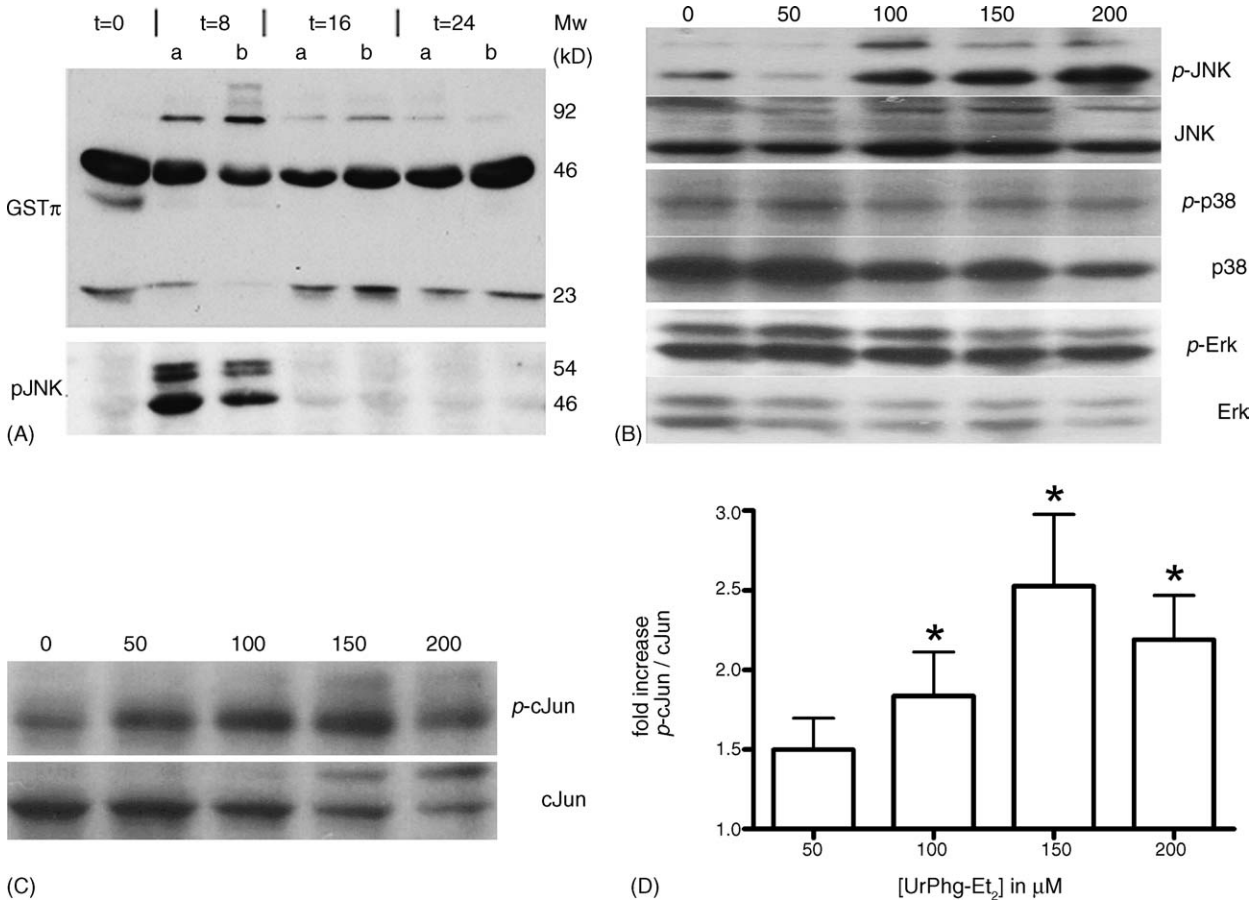

Fig. 4 – UrPhg-Et$_2$ induces GSTπ oligomerization and JNK activation: (A) MTLn3 cells were exposed to 50 μM UrPhg-Et$_2$ (a) or 25 μM γGCP (b) for indicated times. GSTπ oligomerization state (upper panel) was determined by Western blotting under non-denaturing conditions, JNK phosphorylation was analyzed by standard (denaturating) Western blotting. (B) MTLn3 cells were exposed for 4 h to indicated concentrations (in μM) of UrPhg-Et$_2$, after which cell lysates were used for Western blot analysis. (C) MTLn3 cells were exposed to increasing concentrations of UrPhg-Et$_2$ for 4 h, after which lysates were analyzed for cJun phosphorylation by Western blot. (D) Densitometric analysis of three separate (phospho)cJun Western blot experiments. Shown are mean ± S.E.M. of the *p*-cJun/cJun ratio, symbol '*' indicates significant increase compared to the control (Student *t*-test, d.f. = 4, $p < 0.05$)).

in MTLn3 cells. Under non-denaturating conditions, GSTπ is predominantly present as non-covalently linked homodimers; the 46 kDa dimer was therefore the main band (Fig. 4A); this band also includes covalent GSTπ dimers formed by inter-subunit disulfide bonding of GSTπ monomers (Mw 23 kDa). Additional bands at 21 and 37 kDa were detected, presumably corresponding to post-translationally modified GSTπ [35]. After UrPhg-Et$_2$ exposure, bands at 92 kDa and higher appear, comprised of four or more GSTπ subunits. After 16 h, GSTπ oligomerization is lost. In concordance with GSTπ oligomerization, UrPhg-Et$_2$ exposed MTLn3 cells also display a strong increase in JNK phosphorylation. Phospho-JNK levels return to base-levels 16 h after exposure. Altogether this shows that UrPhg-Et$_2$ is able to induce GSTπ oligomerization and JNK activation, albeit transiently.

To assess the effects of short-term exposure to UrPhg-Et$_2$, we investigated phosphorylation of JNK, Erk and p38 by immunoblot. Fig. 4B clearly shows that GSTπ inhibition concentration-dependently induces JNK phosphorylation.

Table 3 – Modulation of the cytostatic effect of thiotepa, cisplatin and doxorubicin by UrPhg-Et$_2$

	IC_{50} (μM)		
	[UrPhg-Et$_2$] = 0	[UrPhg-Et$_2$] = 25	[UrPhg-Et$_2$] = 50
MCF7			
Thiotepa	164 ± 26	152 ± 11	77 ± 8
Cisplatin	34 ± 4	17 ± 2	8 ± 1
Doxorubicin	7 ± 3	5 ± 0.8	2 ± 0.5
VCREMS			
Thiotepa	1380 ± 170	766 ± 59	223 ± 29
Cisplatin	115 ± 16	93 ± 16	23 ± 4
Doxorubicin	11 ± 1	7 ± 0.6	4 ± 0.6

Shown are IC_{50} values (μM, ±S.E.M., $n = 3$).

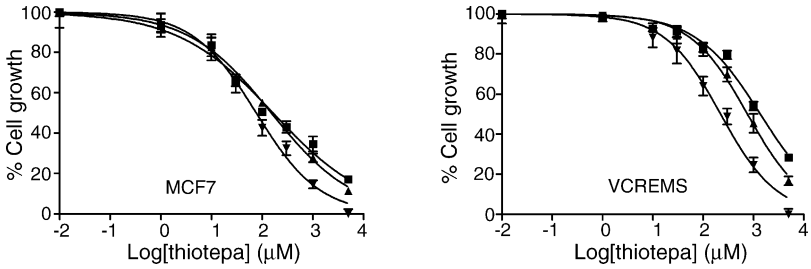

Fig. 5 – UrPhg-Et_2 modulates thiotepa cytotoxicity in breast cancer cell lines. Shown are representative dose–response curves (mean ± S.E.M., $n = 3$) showing inhibition of MCF7 and VCREMS cell growth by thiotepa in the presence or absence of 0 (■), 25 μM (▲) or 50 μM (▼) UrPhg-Et_2. Cells were exposed to thiotepa/UrPhg-Et_2 during 4 h and cell proliferation was determined after 72 h.

This is rather unexpected: although dissociation of monomeric GSTπ facilitates the kinase function of JNK, its phosphorylation must be caused by activation of SEK1 or factors even further upstream in the JNK signaling module. Activation of MAPK signaling seems restricted to the JNK pathway; in contrast to JNK, the other MAPK family members p38 and Erk are not phosporylated in response to UrPhg-Et_2.

As shown, GSTπ inhibition initiates JNK-mediated signaling. The penultimate event in this cascade is JNK-induced phosphorylation of transcription factors, such as cJun and ATF2, which will subsequently regulate transcription of target genes through binding to their respective promoters. As shown in Fig. 4C and D, cJun phoshorylation increases during a short-term exposure to UrPhg-Et_2.

3.4. *Modulation of antineoplastic drug cytotoxicity through GSTP1-1 inhibition*

UrPhg competitively inhibits GSTπ, induces JNK signaling and may also modulate GSTπ-mediated drug resistance. Hereto we used MCF7 derived VCREMS human breast tumor cells, which display increased resistance towards a variety of anticancer agents [36]. VCREMS cells express high levels of GSTπ and *p*-glycoprotein, both of which are low in MCF7. As model antineoplastic agents, we used thiotepa, cisplatin and doxorubicin. We exposed cells for 4 h to the cytostatics in the presence of UrPhg-OEt_2 and determined cell proliferation after 72 h. IC_{50} values, shown in Table 3, were determined from dose–response curves (as shown for thiotepa in Fig. 5) to assess the effect of the GST inhibitor on antineoplastic drug cytotoxicity. The multidrug resistant VCREMS cell line was highly resistant to thiotepa and, to lesser extend, to cisplatin and doxorubicin, when compared to parent MCF7 cells. Co-incubation with UrPhg-OEt_2 enhanced cytotoxicity of all three cytostatics in both cell lines.

4. Discussion

In the present study, we evaluated inhibitory potency of a series of peptidomimetic GSH conjugate analogs towards recombinant human GST isoenzymes. One of these peptidomimetic linkages was then used to obtain a GSTπ selective inhibitor. We showed that this compound promotes the cytostatic effect of several anticancer agents. In addition, it induces phosphorylation of JNK and its downstream target cJun.

Glutathione conjugation, catalyzed by GST, is a major event in the sequestration of electrophiles. GSH conjugates are then readily excreted by members of the MRP family of efflux-pumps. Both GST and MRP are frequently overexpressed in multidrug resistant tumors, acting either alone or in concert [8]. GSH conjugates are potent inhibitors of both these GSH dependent enzymes and, by disturbing GSTπ–JNK interactions, can also influence gene transcription. A major drawback of GSH conjugates is their inherit lability towards γGT, which limits their use in vivo. To address this problem, we employed peptide-bond surrogates to fortify the γ-Glu–Cys amide. We recently reported the inhibition of MRP1 by these compounds and demonstrated the ability of Ur(EA) to abolish MRP1-mediated resistance to methotrexate in ovarian carcinoma cells [24]. For our present study, the effects of peptide backbone alterations on GST inhibition was evaluated with a panel of recombinant human GSTs. The peptidomimetic GSH-analogs were conjugated to ethacrynic acid (EA), as GS-EA is a potent inhibitor these GSTs. Molecular modeling studies showed that the EA moiety binds to the hydrophobic binding site (H-site) of GSTs in a similar fashion for all GS-EA mimics (not shown); differences in binding efficacy, therefore, reflects altered affinity for the peptide portion of the molecules. The shape and electronic configuration of the GSH binding site (G-site) is relatively conserved among the different GST isoenzymes; GSH is bound in strikingly similar fashion in different isoenzymes. This is surprising because there are only few similarities in the amino acid residues that form the G-site [37]. For GSH, the main contributors to G-site docking are the terminal glycine carboxyl and the zwitterionic glutamic acid residue [38,39]. Furthermore, H-bonding interactions with the GSH amides are essential for binding and keeping GSH in an optimal bioactive conformation. As a result, alterations in the GSH peptide backbone can dramatically alter binding characteristics, as was seen for some of our GS-EA mimics (for example, MeCys(EA)). A urethane-type amide proved to be well accepted by GSTs. As Ur(EA) also potently inhibits MRP1 [24], it is a potential candidate for the development of a multiple target MDR-modifier. We utilized the urethane peptide-bond mimic of Ur(EA) together with a phenylglycine moiety to obtain a GSTπ selective inhibitor.

Elevated expression of GSTπ, either alone or coordinately with MRP1, generates resistance towards alkylating antineoplastic drugs, but also towards other drug classes. This is a controversial observation; GSTπ-mediated resistance has also been reported for etoposide, doxorubicin and other cytostatics which are not substrates for GSTπ. For our experiments, we used VCREMS cells, which display elevated amounts of GSTπ and *p*-glycoprotein as a result of mutagenesis with ethyl methane sulfonate and subsequent selection with vincristin [36]. The parent cell line MCF7 expresses low levels of GSTπ. VCREMS cells were originally characterized as resistant towards doxorubicin, vincristin and etoposide, but not to cisplatin. In our experiments, we actually did observe a decreased sensitivity towards this platinum drug. In general, coexposure with UrPhg-Et_2 sensitizes the breast cancer cells to thiotepa, cisplatin and doxorubicin. As this effect is also seen in MCF7 cells, questions arise whether the increased drug sensitivity is due to obstruction of GST enzyme activity. The effects of UrPhg-Et_2 on JNK-mediated signaling provides a more likely explanation. Studies have shown that cisplatin and doxorubicin induced cell killing is dependent on prolonged JNK activity; JNK inhibition delays the onset of cisplatin induced apoptosis [40]. UrPhg-Et_2 may induce the dissociation of GSTπ from JNK and facilitate its kinase function, thereby improving the apoptotic response after cytostatic insult. Regulation of JNK-mediated signaling through its interaction with GSTπ provides an explanation for many of the controversies regarding GSTπ expression and MDR [41]. The GST–JNK interaction can be perturbed either by oxidative stress or by binding of an inhibitor in the GSTπ active site, which induces a conformational change of the enzyme. We showed that UrPhg-Et_2 induces GSTπ oligomerization, which may represent a fraction of the enzyme that has dissociated from JNK. In addition, GSTπ cluster formation is accompanied by JNK activation, which eventually leads to cJun phosphorylation. Unknown is why JNK becomes phosphorylated. Adler et al. showed that phosphorylation of JNK by MKK4 is not inhibited by GSTπ, although forced expression of GSTπ reduces the phosphorylation level of MKK4 itself [10]. An excess of GSTπ may block the MKK4-JNK module, which can be cleared by GSTπ inhibitors. In this scenario, UrPhg-Et_2 could be able to induce JNK phosphorylation. Remarkably, UrPhg-Et_2 does not promote p38 and Erk phosphorylation. HL60 cells, chronically exposed to TLK199, show elevated levels of phospho-Erk [42]. This was also seen in embryonic fibroblast derived from GSTπ−/− mice. Our data suggest that Erk activation by GSTπ inhibitors is not seen after a short-term exposure, and may therefore reflect a secondary response to the initial JNK activation. Indeed, UrPhg-Et_2 induced JNK activity gives rise to phosphorylation of cJun, which is also responsible for the immunoproliferative effect of TLK199 in vivo. We, therefore, speculate that UrPhg-Et_2 might cause a similar response in vivo, which may be clinically relevant. The mechanism behind this event is not completely understood, although it has been shown that deregulation of JAK/STAT signaling is a crucial event for increased myeloproliferation in GSTπ−/−mice [43]. Gene expression profiling after GSTπ inhibitor exposure may provide more information regarding the consequences of GSTπ inhibition on (tumor) cell biology.

All together, our data show that GSH conjugate analogs that contain peptide-bond isosteres can be used as isoenzyme selective GST inhibitors. The improved peptidase stability may be beneficial in vivo. Such compounds are of pharmaceutical interest, as they can manipulate anticancer drug sensitivity and cell biological processes. Using our peptide-bond mimetics, selective inhibitors can be devised for GST, MRP1, glyoxalase, DNA-dependent protein kinase (DNA-pk) and presumably also for numerous other GSH-dependent enzymes.

Acknowledgements

This work was financially supported by the Dutch Cancer Society, grant RUL2002-2741. We thank Dr. Roland Wolff (Ninewells Hospital and Medical School, Dundee, Scotland) for providing VCREMS cells.

REFERENCES

[1] Armstrong RN. Structure, catalytic mechanism, and evolution of the glutathione transferases. Chem Res Toxicol 1997;10:2–18.
[2] Tsuchida S, Sato K. Glutathione transferases and cancer. Crit Rev Biochem Mol Biol 1992;27:337–84.
[3] Whalen R, Boyer TD. Human glutathione S-transferases. Semin Liver Dis 1998;18:345–58.
[4] Mannervik B, Danielson UH. Glutathione transferases-structure and catalytic activity. CRC Crit Rev Biochem 1988;23:283–337.
[5] Hayes JD, Pulford DJ. The glutathione S-transferase supergene family: regulation of GST and the contribution of the isoenzymes to cancer chemoprotection and drug resistance. Crit Rev Biochem Mol Biol 1995;30:445–600.
[6] Board PG, Coggan M, Chelvanayagam G, Easteal S, Jermiin LS, Schulte GK, et al. Identification, characterization, and crystal structure of the Omega class glutathione transferases. J Biol Chem 2000;275:24798–806.
[7] Tew KD. Glutathione-associated enzymes in anticancer drug resistance. Cancer Res 1994;54:4313–20.
[8] Morrow CS, Smitherman PK, Townsend AJ. Combined expression of multidrug resistance protein (MRP) and glutathione S-transferase P1-1 (GSTP1-1) in MCF7 cells and high level resistance to the cytotoxicities of ethacrynic acid but not oxazaphosphorines or cisplatin. Biochem Pharmacol 1998;56:1013–21.
[9] Satoh K. Weak electrophile selective characteristics of the rat preneoplastic marker enzyme glutathione S-transferase P-form, GST-P (7-7): a theory of linear free energy relationships for evaluation of the active site hydrophobicity of isoenzymes. Carcinogenesis 1998;19:1665–71.
[10] Adler V, Yin Z, Fuchs SY, Benezra M, Rosario L, Tew KD, et al. Regulation of JNK signaling by GSTp. EMBO J 1999;18:1321–34.
[11] Wang T, Arifoglu P, Ronai Z, Tew KD. Glutathione S-transferase P1-1 (GSTP1-1) Inhibits c-Jun N-terminal kinase (JNK1) signaling through interaction with the C terminus. J Biol Chem 2001;276:20999–1003.
[12] Dulhunty A, Gage P, Curtis S, Chelvanayagam G, Board P. The glutathione transferase structural family includes a nuclear chloride channel and a ryanodine receptor calcium release channel modulator. J Biol Chem 2001;276:3319–23.

[13] Ryoo K, Huh SH, Lee YH, Yoon KW, Cho SG, Choi EJ. Negative regulation of MEKK1-induced signaling by glutathione S-transferase mu. J Biol Chem 2004;279: 43589–94.
[14] Burg D, Mulder GJ. Glutathione conjugates and their synthetic derivatives as inhibitors of glutathione-dependent enzymes involved in cancer and drug resistance. Drug Metab Rev 2002;34:821–63.
[15] Morgan AS, Ciaccio PJ, Tew KD, Kauvar LM. Isozyme-specific glutathione S-transferase inhibitors potentiate drug sensitivity in cultured human tumor cell lines. Cancer Chemother Pharmacol 1996;37:363–70.
[16] Chen WJ, deSmidt PC, Armstrong RN. Stereoselective product inhibition of glutathione S-transferase. Biochem Biophys Res Commun 1986;141:892–7.
[17] Ong LK, Clark AG. Inhibition of rat liver glutathione S-transferases by glutathione conjugates and corresponding L-cysteines and mercapturic acids. Biochem Pharmacol 1986;35:651–4.
[18] Clark AG, Debnam P. Inhibition of glutathione S-transferases from rat liver by S-nitroso-L-glutathione. Biochem Pharmacol 1988;37:3199–201.
[19] Hanigan MH. Gamma-glutamyl transpeptidase, a glutathionase: its expression and function in carcinogenesis. Chem Biol Interact 1998;111–112:333–42.
[20] Ouwerkerk-Mahadevan S, Mulder GJ. Inhibition of glutathione conjugation in the rat in vivo by analogues of glutathione conjugates. Chem Biol Interact 1998;111–112:163–76.
[21] Burg D, Filippov DV, Hermanns R, van der Marel GA, van Boom JH, Mulder GJ. Peptidomimetic glutathione analogues as novel gGT stable GST inhibitors. Bioorg Med Chem 2002;10:195–205.
[22] Ploemen JH, van Ommen B, van Bladeren PJ. Inhibition of rat and human glutathione S-transferase isoenzymes by ethacrynic acid and its glutathione conjugate. Biochem Pharmacol 1990;40:1631–5.
[23] Awasthi S, Srivastava SK, Ahmad F, Ahmad H, Ansari GA. Interactions of glutathione S-transferase-pi with ethacrynic acid and its glutathione conjugate. Biochim Biophys Acta 1993;1164:173–8.
[24] Burg D, Wielinga P, Zelcer N, Saeki T, Mulder GJ, Borst P. Inhibition of the multidrug resistance protein 1 (MRP1) by peptidomimetic glutathione-conjugate analogs. Mol Pharmacol 2002;62:1160–6.
[25] Lyttle MH, Hocker MD, Hui HC, Caldwell CG, Aaron DT, Engqvist GA, et al. Isozyme-specific glutathione-S-transferase inhibitors: design and synthesis. J Med Chem 1994;37:189–94.
[26] Habig WH, Pabst MJ, Jakoby WB. Glutathione S-transferases-The first enzymatic step in mercapturic acid formation. J Biol Chem 1974;249:7130–9.
[27] Kakkar T, Boxenbaum H, Mayersohn M. Estimation of Ki in a competitive enzyme-inhibition model: comparisons among three methods of data analysis. Drug Metab Dispos 1999;27:756–62.
[28] Kakkar T, Pak Y, Mayersohn M. Evaluation of a minimal experimental design for determination of enzyme kinetic parameters and inhibition mechanism. J Pharmacol Exp Ther 2000;293:861–9.
[29] Rago R, Mitchen J, Wilding G. DNA fluorometric assay in 96-well tissue culture plates using Hoechst 33258 after cell lysis by freezing in distilled water. Anal Biochem 1990;191:31–4.
[30] Lucente G, Luisi G, Pinnen F. Design and synthesis of glutathione analogues. Farmaco 1998;53:721–35.
[31] Koehler RT, Villar HO, Bauer KE, Higgins DL. Ligand-based protein alignment and isozyme specificity of glutathione S-transferase inhibitors. Proteins 1997;28:202–16.
[32] Keppler D, Leier I, Jedlitschky G, Konig J. ATP-dependent transport of glutathione S-conjugates by the multidrug resistance protein MRP1 and its apical isoform MRP2. Chem Biol Interact 1998;111–112:153–61.
[33] Flatgaard JE, Bauer KE, Kauvar LM. Isozyme specificity of novel glutathione-S-transferase inhibitors. Cancer Chemother Pharmacol 1993;33:63–70.
[34] Ouwerkerk-Mahadevan S, Tirona RG, Ripping RA, Ploemen JH, van Bladeren PJ, Pang KS, et al. Inhibition of glutathione conjugation by glutathione analogues in the perfused rat liver. Effect of esterification on the potency of gamma-L-glutamyl-alpha-(D-2-aminoadipyl)-N-2-heptylamine. Drug Metab Dispos 1997;25:1137–43.
[35] Shen H, Tsuchida S, Tamai K, Sato K. Identification of cysteine residues involved in disulfide formation in the inactivation of glutathione transferase P-form by hydrogen peroxide. Arch Biochem Biophys 1993;300:137–41.
[36] Whelan RD, Waring CJ, Wolf CR, Hayes JD, Hosking LK, Hill BT. Over-expression of *p*-glycoprotein and glutathione S-transferase pi in MCF-7 cells selected for vincristine resistance in vitro. Int J Cancer 1992;52:241–6.
[37] Wilce MC, Parker MW. Structure and function of glutathione S-transferases. Biochim Biophys Acta 1994;1205:1–18.
[38] Oakley AJ, LoBello M, Battistoni A, Ricci G, Rossjohn J, Villar HO, et al. The structures of human glutathione transferase P1-1 in complex with glutathione and various inhibitors at high resolution. J Mol Biol 1997;274:84–100.
[39] Oakley AJ, Rossjohn J, LoBello M, Caccuri AM, Federici G, Parker MW. The three-dimensional structure of the human Pi class glutathione transferase P1-1 in complex with the inhibitor ethacrynic acid and its glutathione conjugate. Biochemistry 1997;36:576–85.
[40] Krilleke D, Ucur E, Pulte D, Schulze-Osthoff K, Debatin KM, Herr I. Inhibition of JNK signaling diminishes early but not late cellular stress-induced apoptosis. Int J Cancer 2003;20(107):520–7.
[41] Tew KD, Ronai Z. GST function in drug and stress response. Drug Resist Updat 1999;2:143–7.
[42] Ruscoe JE, Rosario LA, Wang T, Gate L, Arifoglu P, Wolf CR, et al. Pharmacologic or genetic manipulation of glutathione-S-transferase pi influences cell proliferation pathways. J Pharmacol Exp Ther 2001;298:339–45.
[43] Gate L, Majumdar RS, Lunk A, Tew KD. Increased myeloproliferation in glutathione S-transferase pi-deficient mice is associated with a deregulation of JNK and Janus kinase/STAT pathways. J Biol Chem 2004;279:8608–16.